Bis(9-borabicyclo[4.2.1]nonanes)[1)]

Mohamed Yalpani*[a], Roland Boese[b], and Roland Köster[a]

Max-Planck-Institut für Kohlenforschung[a],
Kaiser-Wilhelm-Platz 1, D-4330 Mülheim an der Ruhr

Insitut für Anorganische Chemie der Universität Essen[b],
Universitätsstraße 5–7, D-4300 Essen

Received July 31, 1987

Solutions of bis(9-borabicyclo[3.3.1]nonane) $(\mathbf{1})_2$ at 150°C in the presence of quinuclidine (**Q**) yield the 1:1 adducts quinuclidine-9-borabicyclo[3.3.1]nonane (**Q-1**) and quinuclidine-9-borabicyclo[4.2.1]nonane (**Q-2**) which after rapid cooling are separable by fractional crystallization. The differing intermolecular interactions found in the crystalline amine-boranes **Q-1** and **Q-2** (X-ray analyses) reflect some of their solid state properties. From **Q-2** on reaction with diethyl ether–BF_3 approximately equimolar mixture of *syn*- and *anti*-bis(9-borabicyclo[4.2.1]nonane) $(\mathbf{2})_2$ is obtained. **Q-2** and therefore $(\mathbf{2})_2$ are also preparable by adding **Q** to the initial hydroboration product mixture obtained from 1,5-cyclooctadiene (**3**) and tetrahydrofuran–BH_3.

Bis(9-borabicyclo[4.2.1]nonane)[1)]

Aus gelöstem Bis(9-borabicyclo[3.3.1]nonan) $(\mathbf{1})_2$ erhält man in Gegenwart von Chinuclidin (**Q**) bei ca. 150°C die 1:1-Additionsverbindungen Chinuclidin-9-Borabicyclo[3.3.1]nonan (**Q-1**) und Chinuclidin-9-Borabicyclo[4.2.1]nonan (**Q-2**), die nach raschem Abkühlen durch fraktionierende Kristallisation voneinander getrennt werden. Im kristallinen **Q-1** und **Q-2** treten unterschiedliche intermolekulare Wechselwirkungen auf (Röntgenstrukturanalysen), durch die einige Festkörpereigenschaften der Amin-Borane **Q-1** und **Q-2** erklärt werden. Aus **Q-2** läßt sich mit Diethylether–BF_3 ein etwa äquimolares Gemisch von *syn*- und *anti*-Bis(9-borabicyclo[4.2.1]nonan) $(\mathbf{2})_2$ herstellen. **Q-2** und $(\mathbf{2})_2$ sind aus dem bei 20°C hergestellten Hydroborierungsgemisch von 1,5-Cyclooctadien (**3**) mit Tetrahydrofuran–BH_3 nach unmittelbar erfolgtem Zusatz von **Q** präparativ zugänglich.

In previous reports[2)] we have shown that the internal 1,5-octanediylborane bridge in bis(9-borabicyclo[3.3.1]nonane) [(9-BBN)$_2$, $(\mathbf{1})_2$] is thermally unstable and as a result of a fast mono-dehydroboration-hydroboration exists in equilibrium with 9-borabicyclo[4.2.1]nonane (9-iso-BBN, **2**). The latter, although very early in the history of $(\mathbf{1})_2$[3)] was proposed to be one of the two initial hydroboration products formed in the reaction of THF–BH_3 with 1,5-cyclooctadiene (**3**)[4)], has never been isolated and characterized. Capitalizing on the reactions of tertiary amines with boranes to form stable adducts we hoped to arrive at $(\mathbf{2})_2$ through its amine adduct[5)]. Herein we report on the preparation of $(\mathbf{2})_2$ and its spectroscopic properties. We also describe results which show that the bicyclic compounds **1** and **2** are not always the initial "cyclic" hydroboration products of **3** as variously proposed[4,6)].

Results and Discussion

Preparation of Q-1 and Q-2 from $(\mathbf{1})_2$

Heating a solution of $(\mathbf{1})_2$ in a high boiling hydrocarbon solvent such as mesitylene with two molar quantities of quinuclidine (**Q**) to about 150°C and subsequent rapid cooling gives a crystalline mass in which two crystal modifications are discernible. The ^{11}B-NMR spectrum at 100°C of this solid showed two doublet signals centred at δ 5.0 and 2.8. Fractional crystallization from hexane gives colourless needles of **Q-2** and colourless platelets of **Q-1**. Both solids have nearly identical 70-eV mass spectra and elemental analyses but non-identical infrared spectra. Pure **Q-2** melts at 171–172°C and pure **Q-1** at 165–166°C. However once melted both have a common reduced melting point at 154–156°C. Compound **Q-1** was shown by comparison (IR, ^{11}B NMR, and ^{13}C NMR) to be identical to the product obtained from heating a hexane solution of $(\mathbf{1})_2$ and **Q** for a short time. The ^{13}C-NMR spectrum of the C_8H_{14} bicyclic ring of **Q-1** shows five signals in the ratio of 2:1:1:2:2 while in **Q-2** four signals in the ratio 2:2:2:2 are observed. These are in agreement with a structural assignment with a [3.3.1] bicyclic ring in **Q-1** and [4.2.1] in **Q-2**. The X-ray structure analyses performed on these amine-boranes confirmed these assignments and also revealed interesting aspects of the solid state properties of these isomeric compounds.

Molecular Structures of Q-1 and Q-2

Figure 1 shows the molecular structure of **Q-1**[7)] with basic features similar to those of $(\mathbf{1})_2$[8)] and to the quinuclidine adduct of bis(9-borabicyclo[3.3.1]nonane) oxide[9)].

The structure of **Q-2** is depicted in Figure 2 and shows the bicyclic [4.2.1] ring system as an adduct of quinuclidine.

The noteworthy structural features are: the puckered seven-membered ring segment in which the effects of strain are clearly evident in the widening of the bond angles in this ring segment, the significant elongations of some of the C–C and B–C bond lengths (cf. Table 1), and also in the large quasi 1,3-diaxial interactions of the ring H atoms, some of which (e.g. H3a–H5b, H2b–H7a, and H6a–H8b, cf. Figure 2) have been forced to approach to a distance of less than about 2.3 Å, i.e., within the van der Waals radii of each other. Finally the position of the **Q** moiety on the boron atom at the five-membered ring side of the bicyclic

  0009–2940/88/0202–0287 $ 02.50/0

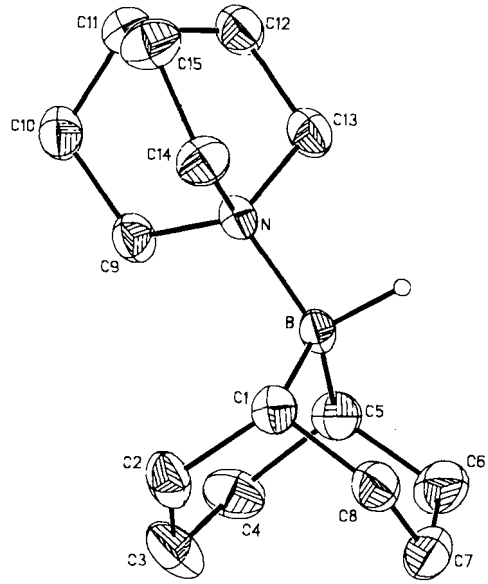

Figure 1. Molecular structure of **Q-1** with all but the hydridic hydrogen atoms at the carbons omitted

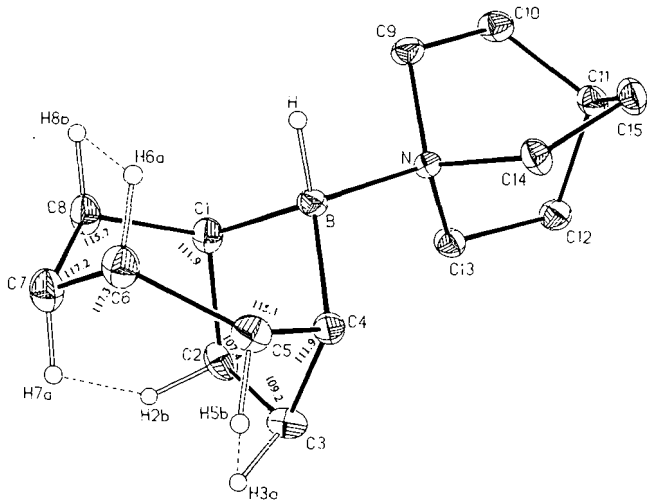

Figure 2. Molecular structure of **Q-2** with selected CCC bond angles and displaying the hydridic as well as hydrogen atoms with intramolecular H···H distances shorter than 2.3 Å

Table 1. Selected bond distances (Å) of **Q-1** and **Q-2**

	Q-1	Q-2		Q-1	Q-2
C1 - C2	1.524(4)	1.565(3)	C7 - C8	1.527(4)	1.542(3)
C2 - C3	1.515(4)	1.551(3)	C8 C1	1.540(4)	1.546(3)
C3 - C4	1.537(4)	1.554(3)	C1 - B	1.613(3)	1.633(3)
C4 C5	1.551(4)	1.541(3)	C4 - B	-	1.646(3)
C5 - C6	1.537(4)	1.531(3)	C5 - B	1.612(3)	-
C6 - C7	1.517(4)	1.525(3)	N - B	1.676(3)	1.663(3)
			C C(av)	1.530(4)	1.544(3)

[4.2.1] system (*exo*-**Q-2**) causes the tilting of the triangular plane comprising the atoms C1, B, and C4 towards the larger ring resulting in an interplanar angle of 104.5° with the plane comprising the atoms C1, C8, C5, and C4.

Selected bond lengths in **Q-1** and **Q-2** are shown in Table 1.

The formation and stability in the solid of **Q-2**, despite the strains in the bicyclic [4.2.1] ring system, must be seen in the advantageous crystal packings as reflected in the higher melting point and also lower solubility of **Q-2** in nonpolar solvents as compared to that of **Q-1**. A comparative analysis of the packings of molecules of **Q-1** and **Q-2** in their respective crystal lattices was therefore expected to reveal the forces underlying this added lattice stability for **Q-2**.

The molecular packings of **Q-1** and **Q-2** are shown as stereo plots in Figures 3a and 3b, respectively.

Figures 4a and 4b exhibit expanded views of these and show that both **Q-1** and **Q-2** are packed in a head to tail fashion such that their central dipolar regions as a result of the tetravalency of the nitrogen and boron atoms, are in a position to exert mutual attractions.

In **Q-1** both of the hydridic hydrogen atoms of a pair neighbouring molecules point towards the centre of the positive charge of the tertiary amine nitrogen of the neighbour. The intermolecular distance between H^B and N′ amounts to about 4.0 Å. This pair, which through the mutual coulombic attractions form discrete entities in the lattice is attracted to the neighbouring pairs by van der Waals' forces. In **Q-2**, on the other hand, the arrangement of the hydridic hydrogen atom of one molecule towards the neighbouring molecule is such that the charge attraction extends from one to the next molecule in the lattice resulting in a quasi ionic polymer. Although the intermolecular H^B-N' distance of about 4.5 Å is much longer in **Q-2** (see Figure 4b), the extension of the attractive forces throughout the lattice is apparently sufficient to shrink the lattice of **Q-2** (density 1.22 g/cm^3) compared to that of **Q-1** (1.14 g/cm^3) and thereby lead to the greater stability of the former as reflected in the high melting point and lower solubility of crystals of **Q-2**. It should be expected that this gain of stability is lost in the free borane. Below we shall see that this is indeed the case.

Formation of *syn*/*anti*-$(2)_2$

On dissolution of **Q-2** in a large portion of hexane at room temperature and treatment with diethyl ether-trifluoroborane a two-phase solution resulted. From the supernatant hexane phase, on evaporation of the solvent in vacuo, a colourless solid $(2)_2$, was obtained. Recrystallization gave prisms melting in a broad range starting at about 120°C. A differential scanning calorimetric analysis (cf. Figure 5) showed an exothermic reaction commencing at about 80°C to be responsible for the broad melting range observed.

This instability of crystals of $(2)_2$ is also observable at room temperature. After several weeks the infrared spectrum, which initially indicates significant differences to that of $(1)_2$, becomes identical to that of the latter.

The mass spectrum of $(2)_2$ is similar to that of $(1)_2$ differing mainly in the intensities of the molecular ion peaks at *m/z* 244 [15% for $(2)_2$; 60% for $(1)_2$ of the respective base peaks at *m/z* 94]. This decrease of the intensity of the molecular ion peak of $(2)_2$ relative to that of $(1)_2$ is a reflection of the

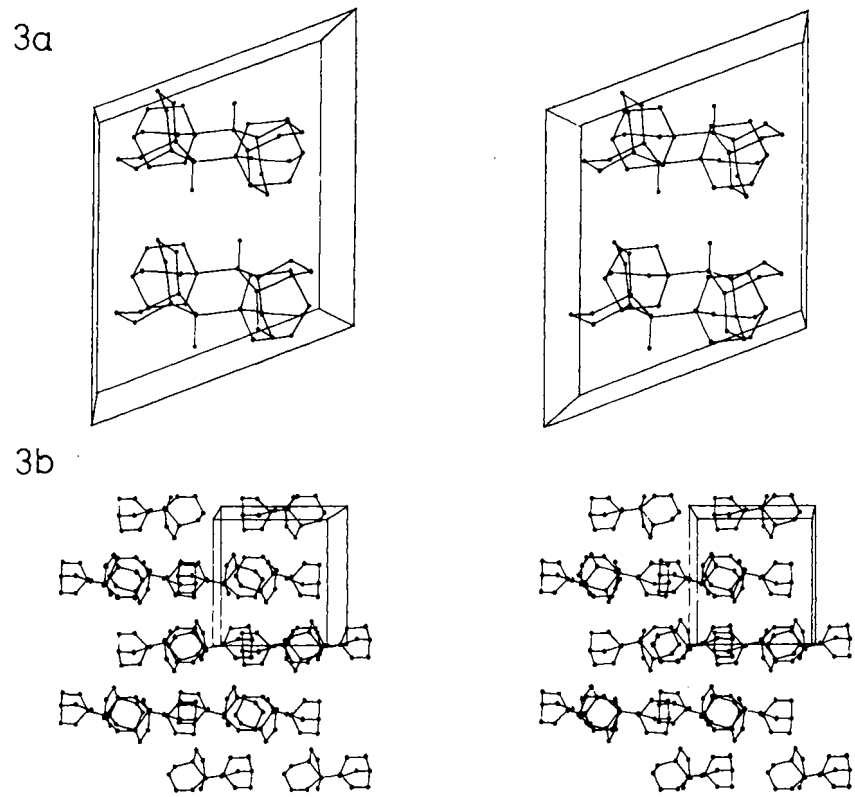

Figure 3a + b: Stereoscopic views of molecular packings of **Q-1** and **Q-2** respectively

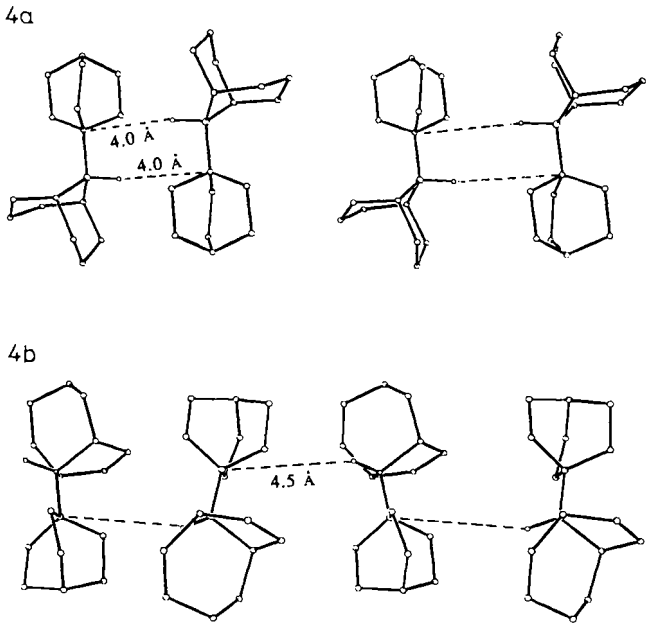

Figure 4a + b: Display of intermolecular interactions of **Q-1** and **Q-2** in their respective crystal lattices

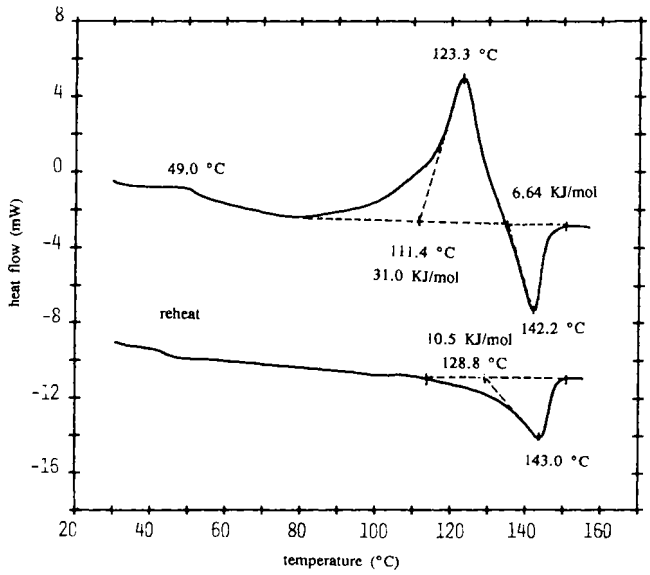

Figure 5. DSC scan of crystalline *syn/anti*-$(\mathbf{2})_2$

weaker diborane(6) bonds bridging the two halves of $(\mathbf{2})_2$, a fact which is also evident in the slight shift of the infrared absorption band for the $>BH_2B<$ bond from 1567 cm^{-1} in $(\mathbf{1})_2$[10] to 1550 cm^{-1} in $(\mathbf{2})_2$. Finally the ^{13}C-NMR spectrum of $(\mathbf{2})_2$ obtained at $-30°C$ [to avoid slow conversion at room temperature to $(\mathbf{1})_2$] can be interpreted to show the presence of both of the *syn* and *anti* geometric isomers of $(\mathbf{2})_2$.

From the integral intensities of the ^{13}C-NMR signals it can be seen that one of the isomers is sligthly more stable at $-30°C$. Leaving the NMR sample in a toluene solution

at room temperature for several days results in an intermediate spectrum showing the presence of a mixture of $(\mathbf{1})_2$, (**1-2**), and $(\mathbf{2})_2$. On further standing of the solution at room temperature only the signals corresponding to that of $(\mathbf{1})_2$ are found. The steps leading to $(\mathbf{2})_2$ are shown in Scheme 1.

Scheme 1. Reaction pathways to **Q-1**, **Q-2**, and *syn/anti*-$(\mathbf{2})_2$

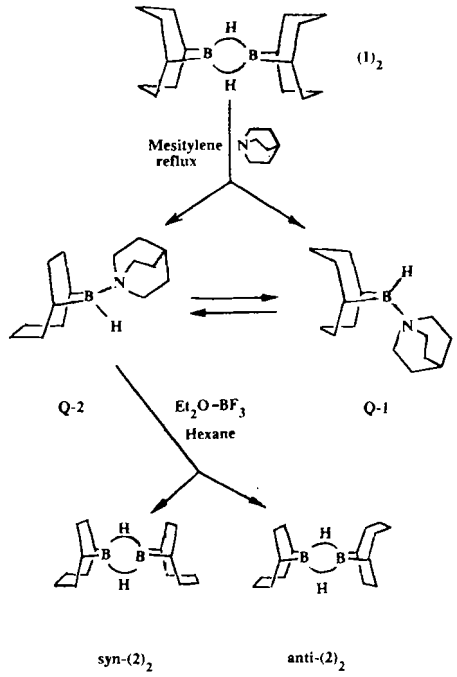

Hydroboration of 3

a) With $THF-BH_3$

The success in isolating $(\mathbf{2})_2$ via **Q-2** from $(\mathbf{1})_2$ at 150°C suggested the possibility of also isolating **2** as **Q** adduct at low temperatures and so varying its proposed[4] formation as an intermediate in the course of the synthesis of $(\mathbf{1})_2$ from **3** and $THF-BH_3$.

Thus, when stoichiometric amounts of **Q** was added to the solution, e. g. in toluene, of the product mixture resulting from the room-temperature addition of **3** to $THF-BH_3$ immediately after the initial reaction only a 40% yield of the expected crystalline adduct mixture of **Q-1** and **Q-2** was obtained. From this mixture pure **Q-2** could be separated by fractional crystallization. When **Q** was added to the hydroboration product mixture after the latter had been stirred at room temperature for several hours the **Q** adduct formation was about quantitative, consisting however of nearly pure **Q-1**. This discrepancy suggested that either the hydroboration was initially incomplete or that besides $(\mathbf{1})_2$ and $(\mathbf{2})_2$ other products are also formed which slowly convert to $(\mathbf{1})_2$. A ^{11}B-NMR study of the hydroboration of **3** with $THF-BH_3$ had shown the formation of various intermediates among which some gave rise to signals assignable to trialkylboranes[11]. A ^{11}B-NMR spectrum of our initial hydroboration mixture shows two major signals at 27.6 and 82 ppm with the integral ratio of 5:7.

The peak at 27.6 ppm corresponds to $(\mathbf{1})_2$ or $(\mathbf{2})_2$, the larger broad signal, centred at about 82 ppm, can be attributed to trialkylboranes. The broadness of this signal suggests polymeric organoboron compounds. The ^{13}C-NMR spectrum of the same initial hydroboration mixture is also a reflection of the complex nature of the products. The ^{13}C-NMR signals corresponding to $(\mathbf{1})_2$ and $(\mathbf{2})_2$ can be identified, these are, however, only present as minor components.

The presence of major amounts of trialkylboranes in the initial reaction mixture explains the low yield of the **Q** adduct found but appear to contradict the "cyclic hydroboration" mechanism occasionally propounded[6]. We proceeded to further scrutinize this reaction. The procedure of choice to arrive at the conclusions resulting in the proposal of the "cyclic" nature of hydroboration of dienes has been the alkaline hydrogen peroxide oxidation of the hydroboration products and the gas-chromatographic analysis of acetate derivatives of the resulting diols[6]. Using the same methods the results for reactions carried out at various conditions, e. g., mode of addition, reaction temperature, and molar ratio of reactants, are shown in Table 2.

Table 2. Hydroboration of 1,5-cyclooctadiene (**3**) with $THF-BH_3$ or Et_2BH

Exp. No	mmol 3	mmol $THF-BH_3$	mmol Et_2BH	temp. °C	cyclooctanedioldiacetates*) (Rel.%) trans 1,4-	trans 1,5-	cis 1,5-	cis 1,4-
1	27.08*)	30.30	–	30	37.0	11.0	24.0	28.0
2	76.72	76.91*)	–	30	44.5	13.0	10.0	32.4
3	39.50	122.61*)	–	30	46.9	12.3	9.4	31.3
4	30.59	94.70*)	–	0	0.3	0.5	68.7	30.2
5	31.80*)	32.33	–	0	2.3	6.7	58.5	32.6
6	32.56	38.30*)	–	-15	0.4	0.2	67.9	32.0
7	47.12*)	–	154.20	~ 40	35.6	5.5	18.0	41.0
8	78.20	–	306.00*)	~ 40	53.7	11.7	11.2	23.4
9**)	39.20*)	–	150.30	0	5.1	14.9	10.5	14.2
9a***)	39.20*)	–	150.30	30/2h	22.4	36.5	17.5	23.6

*) Reagent that was added dropwise to the reaction mixture. – **) In this reaction the main oxidation product was the 1,3-diol (55.2%). – ***) The reaction product of experiment 9 was warmed to 30°C and stirred for 2 h. – +) Analyzed by GC.

It is seen that independent of addition mode of the reactants, both the *trans*- as well as the *cis*-1,4- and -1,5-diols are the oxidation products of the hydroboration mixture at 30°C (see Table 2, Exp. 1–3). In the initial hydroboration products obtained at lower temperatures (e. g. –15 to 0°C), however, independent of molar ratios of reactants and mode of addition of the reagents, the signal correponding to trialkylboranes are virtually absent in their ^{11}B- and ^{13}C-NMR spectra and their oxidation products contain largely *cis*-diols (see Table 2, Exp. 4–6).

These results show that the initially formed monohydroborated species **4** (see Scheme 2) can react along more than

one pathway: At lower temperatures the intramolecular reaction gives rapidly $(\mathbf{1})_2$, **1-2**, or $(\mathbf{2})_2$, while at 30°C intermolecular reactions with either excess of **3** or of $THF-BH_3$ to give oligomeric trialkylboranes are competing. These steps are shown in Scheme 2.

Scheme 2. Pathways to 9-borabicyclo[3.3.1]nonane (**1**)

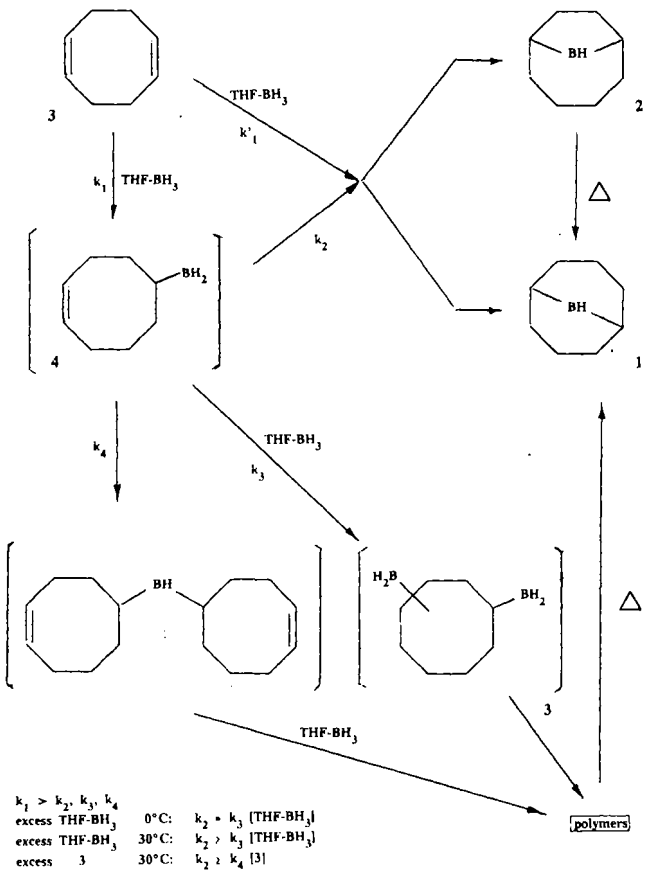

b) With Ethyldiboranes(6)

Finally it was of interest to also investigate and compare the initial stages of the original[3] synthesis of $(\mathbf{1})_2$ using tetraalkyldiborane(6) and **3**. It would be expected that since the predominant species in the borane reagent is R_2BH[12], the initial hydroboration of **3** should lead predominantely to mixtures of trialkylboranes. In fact the presence of the main signals in the ^{11}B-NMR spectrum of the initial product mixture (reaction carried out at 30–40°C, after removal of volatile boranes in vacuo) at δ 26.2, 28.2, and 29.0 (Σ integral intensities > 90%) indicates the presence of tetraalkyldiborane(6) structures. The two small signals at δ 86.5 and 91.5 can be assigned to 9-alkyl derivatives of **1** and **2**, respectively. The ^{13}C-NMR spectrum of this sample showed signals corresponding to $(\mathbf{1})_2$, **1-2**, and $(\mathbf{2})_2$ in small concentrations, as well as, a multitude of signals in the range of δ 26–33. The oxidative workup of the product gave mixtures of *cis*- and *trans*-diols. Reversing the order of addition of the reagents had no significant effect on the composition of the diols (see Table 2, Exp. 7 and 8). Surprisingly, the addition of **3** to tetraethyldiborane(6) at 0°C resulted in the formation of 1,3-diol as the major oxidation product[13]. However, this diol was absent in the oxidation mixture when the reaction solution was first heated to 30°C for 2 h, the *cis*- and *trans*-1,4- and -1,5-diols being present in near statistical ratios (see Table 2, Exp. 9 and 9a).

c) Conclusion

The use of the term "cyclic hydroboration"[6], if it is denoted to the mechanism of the initial reactions of boranes with dienes, is a misleading notion since depending on the reaction conditions varying amounts of noncyclic products are formed when $THF-BH_3$ is used, and cyclic products are also produced when the borane reagent is tetraalkyldiborane(6). This would either mean considerable rearrangement of the reagent prior to the hydroboration step, or of the products thereof which is a more likely assumption. Should, however, the use of this term describe the final rather than the initial products, it should be noted that in most cases, independent of the nature of the latter, fast >B–H catalysed reforming will lead to the thermodynamic stable final cyclic products when the appropriate diene is hydroborated.

Experimental

Instruments: Büchi melting point apparatus, sealed capillary tubes, uncorrected. – DSC analyses: DuPont 1090. – Gas chromatograms[14]: Siemens Sinchromat 1 with a 43-m OV 225 capillary column, injection port at 250°C, oven at 80–200°C, programmed at 8°C/min, helium as carrier gas. – Infrared spectra: Nicolet 7199 FT-IR system. – Mass spectra[14]: MAT CH 5 and 311 A. – ^{1}H-NMR spectra: Varian EM 360 and Bruker WP 200. – ^{11}B-NMR spectra[14]: Varian XL-100, diethyl ether–BF_3 as external standard. – ^{13}C-NMR spectra: Varian XL 100 and Bruker WP 300[14].

Quinuclidine-9-Borabicyclo[3.3.1]nonane (**Q-1**): A solution of 2.5 g (10.4 mmol) of $(\mathbf{1})_2$ and 2.4 g (21.6 mmol) of quinuclidine (**Q**) in 100 ml of hexane was brought for about 5 min to reflux and cooled slowly to –60°C. The colourless platelets of **Q-1** were separated, 4.7 g (97%), m.p. 165–166°C. – ^{1}H NMR ($CDCl_3$): δ = 3.0 (m, 6H); 1.7 (m, 20H); 0.8 (br, 2H). – ^{13}C NMR ($CDCl_3$): Signals for quinuclidine moiety δ 20.4 (d, 1C); 25.0 (t, 3C); 57.2 (t, 3C); signals for **1** moiety δ = 21.9 (br, 2C); 24.3 (t, 1C); 25.8 (t, 1C); 30.1 (t, 2C); 38.0 (t, 2C). – ^{11}B NMR (nonane, 20°C): δ = 2.8 (br, s); (100°C): δ = 2.8 (d, J_{BH} = 96 Hz). – MS (70 eV): *m/z* (%) = 233 (M^+, 22), 176 (20), 124 (100).

$C_{15}H_{28}BN$ (233.2) Calcd. C 77.19 H 12.10 B 4.64
Found C 77.01 H 12.30 B 4.85

Quinuclidine-9-Borabicyclo[4.2.1]nonane (**Q-2**): A solution of 5.0 g (20.8 mmol) of $(\mathbf{1})_2$ and 4.9 g (44.1 mmol) of **Q** in about 50 ml of mesitylene was heated at 150°C for 2 h and then rapidly cooled to room temperature. Further slow cooling to –30°C gave a colourless crystalline mixture of needles and platelets (8.2 g, 85%). These crystals were redissolved in about 50 ml of refluxing hexane. The solution was cooled very slowly to room temperature. The colourless needles were separated by filtration, 3.7 g (39%). A further recrystallization from hexane gave analytically pure crystals of **Q-2**, m.p. 171–172°C. – ^{1}H NMR ($CDCl_3$): δ = 2.9 (m, 6H); 1.5 (br, m, 22H). – ^{13}C NMR ($CDCl_3$): signals for the quinuclidine moiety δ 20.6 (s, 1C); 24.9 (t, 3C); 49.8 (t, 3C); signals for **2** moiety δ = 26.6 (t, 2C); 28.6 (br, 2C); 36.1 (t, 2C); 36.8 (t, 2C). – ^{11}B NMR

(nonane, 20°C): δ = 5.0 (br, s); (100°C): δ = 5.0 (d, J_{BH} = 93 Hz). – MS (70 eV): *m/z* (%) = 233 (M^+, 23), 176 (22), 124 (100).

$C_{15}H_{28}BN$ (233.2) Cacld. C 77.19 H 12.10 B 4.64
Found C 77.31 H 11.92 B 4.81

From the above mother liquor on further cooling to about −10°C a second crop of crystals were obtained consisting of a mixture of **Q-1** and **Q-2**. On slow cooling to −78°C colourless platelets, about 3.5 g (38%), of pure **Q-1** were obtained.

syn/anti-Bis(9-borabicyclo[4.2.1]nonane) [(**2**)$_2$]: To a solution of 1.0 g (4.2 mmol) of **Q-2** in 500 ml of hexane at room temperature was added dropwise with rapid stirring 5.0 g (3.60 mmol) of diethyl ether-trifluoroborane. After 1/2 h the supernatant hexane solution was cooled to −78°C and filtered (P 3 sintered glass funnel). The filtrate was evaporated to dryness in vacuo. The resulting colourless solid (0.61 g) was suspended in about 10 ml of hexane, the solution was filtered and cooled very slowly to −60°C. About 0.3 g (ca. 60%) of colourless prisms of (**2**)$_2$ were obtained, m.p. 120–130°C: see DSC diagram Figure 5. – IR: 1550 cm^{-1} (BH_2B). – ^{13}C NMR ($CDCl_3$): δ 26.0 (br, d); 26.49 (t); 26.53 (t); 32.36 (t); 32.42 (t); 33.63 (t); 34.19 (t);. – ^{11}B NMR ($CDCl_3$): δ = 28.0. – MS (70 eV): *m/z* (%) = 244 (M^+, 15), 122 (47), 94 (100).

$C_{16}H_{30}B_2$ (244.0) Calcd. C 78.75 H 12.39
Found C 78.59 H 12.50

X-Ray Single Crystal Structure Determination of **Q-1** *and* **Q-2** *(General Procedure):* Data collection and calculations were carried out on a Syntex R 3 four-cycle diffractometer with a Nova 3/12 (Data General) Nicolet P 3 and SHELXTL software[15]. The structure solutions were carried out by direct methods, and hydrogen atoms were included as rigid groups (C–H bond lengths at 0.96 Å, C–C–H and H–C–H angles of 109.5°). The isotropic atomic displacement parameters (ADP's) of the H atoms were taken as the 1.2 fold of the orthogonalised U_{ij} tensors of the corresponding C atoms. The hydrogen atoms attached to the boron atoms were located from the difference Fourier synthesis and refined with unique ADP. Structural data for **Q-1** and **Q-2** are shown in Table 3, the atom coordinates in Tables 4 and 5.

Table 3. Structural data for **Q-1** and **Q-2**

	Q-1	Q-2
Formula	$C_{15}H_{28}BN$	$C_{15}H_{28}BN$
Crystal size (mm)	0.48x0.31x0.26	0.23x0.21x0.53
Crystal system	monoclinic	orthorhombic
Space group	$P2_1/c$	$P2_12_12_1$
Z	4	4
a (Å)	10.216(2)	9.546(5)
b (Å)	12.689(3)	10.568(4)
c (Å)	11.517(2)	13.360(6)
β (deg)	110.81(1)	-
T (K)	(293)	(128)
V (Å^3)	1395.6(5)	1347.7(10)
d_{calcd} (g/cm^3)	1.1100(293) 1.1433(128 K)	1.2185(128 K)
μ (cm^{-1})	0.58	0.63
Radiation	Mo K_α	Mo K_α
2θmax (deg)	50	50
Total no. of reflcns	2450	1786
Observed reflcns [$F_o \geq 3.50\sigma(F)$]	1650	1585
R	0.053	0.041
R_w [$w^{-1}=\sigma^2(F)+gF^2$]	0.055	0.043
g	$9\cdot10^{-3}$	$8.9\cdot10^{-3}$
residual electron density (e/Å^3)	0.19	0.22

Table 4. Atomic coordinates (× 10^4) and isotropic displacement parameters (pm^2 × 10^{-1}) for **Q-1**

	x	y	z	U*
N	4274(2)	8943(1)	1789(1)	43(1)
B	6004(3)	9102(2)	2167(2)	45(1)
C(1)	6697(2)	10063(2)	3100(2)	51(1)
C(2)	6798(3)	9866(2)	4435(2)	65(1)
C(3)	7500(3)	8844(2)	5006(2)	85(1)
C(4)	7143(3)	7874(2)	4151(2)	73(1)
C(5)	6938(2)	8082(2)	2770(2)	58(1)
C(6)	8350(3)	8273(2)	2609(3)	79(1)
C(7)	9083(3)	9278(2)	3214(3)	80(1)
C(8)	8143(3)	10248(2)	3000(2)	64(1)
C(9)	3824(2)	8374(2)	2723(2)	57(1)
C(10)	2243(3)	8377(2)	2375(2)	71(1)
C(11)	1564(3)	8736(2)	1040(2)	65(1)
C(12)	2166(3)	8080(2)	249(2)	65(1)
C(13)	3719(2)	8325(2)	600(2)	61(1)
C(14)	3553(2)	9994(2)	1538(2)	61(1)
C(15)	1966(3)	9872(2)	943(3)	77(1)

* Equivalent isotropic U defined as 1/3 of the trace of the orthogonilized U_{ij} tensor.

Table 5. Atomic coordinates (× 10^4) and isotropic displacement parameters (pm^2 × 10^{-1}) for **Q-2**

	x	y	z	U*
N	9216(2)	-64(2)	1874(1)	14(1)
B	10740(2)	211(2)	1312(2)	16(1)
C(1)	11788(2)	-1022(2)	1386(2)	20(1)
C(2)	11442(2)	-1852(2)	457(2)	25(1)
C(3)	10804(2)	-969(2)	-352(2)	23(1)
C(4)	10610(2)	385(2)	101(1)	17(1)
C(5)	11717(2)	1323(2)	-303(2)	21(1)
C(6)	13173(2)	1306(2)	196(2)	23(1)
C(7)	13833(2)	16(2)	394(2)	26(1)
C(8)	13344(2)	-638(2)	1357(2)	24(1)
C(9)	9432(2)	-44(2)	2992(1)	21(1)
C(10)	8101(2)	-469(2)	3546(2)	23(1)
C(11)	6861(2)	-403(2)	2823(2)	21(1)
C(12)	7070(2)	-1425(2)	2025(2)	22(1)
C(13)	8571(2)	-1314(2)	1611(2)	20(1)
C(14)	8180(2)	958(2)	1626(2)	21(1)
C(15)	6891(2)	897(2)	2321(2)	23(1)

* Equivalent isotropic U defined as 1/3 of the trace of the orthogonilized U_{ij} tensor.

General Procedure for the Hydroboration of 1,5-Cyclooctadiene (**3**) *with THF–BH_3 (or Et_2BH):* A 100-ml three necked flask equipped with magnetic stirrer, an immersion thermometer, a dropping funnel, and an argon inlet tube was charged, depending on the mode of choice, with either the borane or **3** in 30 ml of THF. The other reactant being added through the dropping funnel at a rate to maintain a constant reaction temperature. On completion of the addition the solvent and volatiles were removed at high vacuum at 0°C. The residue was stored for further use at −30°C.

Alkaline Hydrogen Peroxide Oxidation of the Organoboranes: About 10 mmol of the hydroboration product was added to a solution of 4 ml of 3 N KOH in 10 ml of THF at 0°C. A solution of 2 ml of 30% aqueous hydrogen peroxide in 5 ml of THF was added dropwise during 10 min. After the initial vigorous reaction subsided the mixture was heated to reflux for 2 h. The product mixture was saturated with anhydrous potassium carbonate, the organic layer separated, dried with magnesium sulfate, and evaporated to dryness. The residue was acetylated in the usual way and the product analysed by gas chromatography. The isomeric diacetates were identified by GC-MS analysis using chemical ionization (ammonia gas) and compared with authentic samples.

CAS Registry Numbers

(**1**)$_2$: 21205-91-4 / *anti*-(**2**)$_2$: 110848-71-0 / *syn*-(**2**)$_2$: 110743-69-6 / **3**: 111-78-4 / **Q**: 100-76-5 / **Q-1**: 70338-08-8 / **Q-2**: 110743-68-5

[1] Part 78 of Boron Compounds; Part 77: R. Köster, Y-H. Tsay. L. Synoradzki, *Chem. Ber.* **120** (1987) 1117.

[2] [2a] R. Köster, M. Yalpani, *J. Org. Chem.* **51** (1986) 3054. – [2b] M. Yalpani, R. Köster, *Chem. Ber.* **120** (1987) 607.

[3] R. Köster, *Angew. Chem.* **72** (1960) 626.

[4] E. F. Knights, H. C. Brown, *J. Am. Chem. Soc.* **90** (1968) 5280.

[5] R. Köster in *Methoden der Organischen Chemie* (Houben-Weyl-Müller), 4th ed., Vol. XIII/3b (R. Köster, Ed.), pp 433f, Thieme, Stuttgart 1983.

[6] [6a] H. C. Brown, E. Negishi, D. L. Burke, *J. Am. Chem. Soc.* **94** (1972) 3561. – [6b] H. C. Brown, E. Negishi, *J. Am. Chem. Soc.* **94** (1972) 3567. – [6c] H. C. Brown, E. F. Knights, C. G. Scouten, *J. Am. Chem. Soc.* **96** (1974) 7765. – [6d] H. C. Brown, E. Negishi, *Tetrahedron* **33** (1977) 2331. – [6e] H. C. Brown, H. K. Mondal, S. U. Kulkarni, *J. Org. Chem.* **42** (1977) 1392. – [6f] H. C. Brown, E. Negishi, W. C. Dickason, *J. Org. Chem.* **50** (1985) 520.

[7] Further details of the crystal structure investigations are available on request from the Fachinformationszentrum Energie Physik Mathematik GmbH, D-7514 Eggenstein-Leopoldshafen 2, on quoting the depository number CSD 52697, the names of the authors, and the journal citation.

[8] [8a] D. J. Brauer, C. Krüger, *Acta Crystallogr., Sect. B*, **29** (1973) 1684. – [8b] R. Köster in *Methoden der Organischen Chemie* (Houben-Weyl-Müller), 4th ed., Vol. XIII/3c (R. Köster, Ed.), p. 447, Thieme Stuttgart 1984.

[9] R. Köster, J. Serwatowski, R. Boese, M. Yalpani, unpublished results.

[10] See ref.[8b], p. 441.

[11] R. Contreras, B. Wrackmeyer, *Z. Naturforsch., Teil B*, **35** (1986) 1236.

[12] R. Köster, G. Griasnow, W. Larbig, P. Binger, *Liebigs Ann. Chem.* **672** (1964) 1.

[13] The information of major of 1,3-cyclooctanediol has also been observed in the alkaline hydrogen peroxide oxidation of the hydroboration products of **3** with either of THF–BH_3, tetraethyldiborane(6) or hexylborane; M. Yalpani, unpublished results.

[14] Department for instrumental analysis, Max-Planck-Institut für Kohlenforschung, Mülheim an der Ruhr.

[15] G. M. Sheldrick, SHELXTL (1981). *An Integrated System for Solving, Refining, and Displaying Crystal Structures from Diffraction Data*, Universität Göttingen.

[214/87]